Pergamon

0301-9322(94)E0028-H

Int. J. Multiphase Flow Vol. 20, No. 4, pp. 691–702, 1994

0301-9322/94 $7.00 + 0.00

MAPS OF MEAN GAS VELOCITY FOR STRATIFIED FLOWS WITH AND WITHOUT ATOMIZATION

L. A. DYKHNO, L. R. WILLIAMS and T. J. HANRATTY
University of Illinois, Urbana, IL 61801, U.S.A.

(Received 20 August 1993; in revised form 29 March 1994)

Abstract—The variation of gas velocity in the streamwise direction was measured for air and water flowing in a horizontal 9.53 cm pipe. Secondary flows are inferred from these measurements. At low gas velocities a stratified pattern with little or no entrainment was observed. Contours of constant velocity suggest the existence of two or more secondary cells, which create an upward flow at the walls and a downward flow at the center in the top part of the pipe. At high gas velocities and at large enough liquid flows, that entrainment is significant, droplet stratification causes a secondary pattern with downward flow at the wall.

Key Words: gas–liquid flow, secondary flow, horizontal flow, velocity profiles, annular flow, stratified flow

1. INTRODUCTION

Gas and liquid flowing in a horizontal pipeline at high gas velocities can assume a configuration in which part of the liquid moves as a layer along the wall and part as droplets entrained in the gas. Because of gravity the height of the liquid in the wall layer changes around the circumference of the pipe. The prediction of this variation and of how a continuous liquid film is maintained on the top part of the wall has been of continuing interest.

Droplets removed from the liquid, in a stratified gas–liquid flow, have been observed to wet the walls of the pipe and to initiate the formation of a continuous wall layer (Lin & Hanratty 1987). However, a number of situations have been cited for which the rate of deposition does not appear to be large enough to account for the thickness of the film at the top of the pipe (e.g. Jacowitz & Brodkey 1964).

Pletcher & McManus (1965) suggested that secondary patterns can exist in the gas phase in horizontal annular flows, because of the variation in interfacial drag caused by a variation of the wave height. They argued that these patterns are associated with a gas drag at the interface that has a circumferential component, which opposes gravitational drainage. This notion has been supported with studies of single-phase flows through ducts with walls of non-uniform roughness (Darling & McManus 1968; Hinze 1973). Darling & McManus used an eccentric thread, in a 9.7 cm pipe, whose height decreased from the bottom of the pipe to the top. A secondary pattern was found which consisted of two cells that had flows upward at the walls and downward in the center. Their strength was about 3.5% of the maximum value of the axial velocity.

The existence of secondary velocity fields in fully-developed turbulent flows through straight pipes of non-circular cross-section, which was established by Nikuradse (1962), has been verified by a number of researchers (Speziale 1982). These flows are such that there is a flow toward the corners. Jayanti *et al.* (1990a) have pointed out that the cross-section through which gas is flowing in horizontal gas–liquid annular flow is non-circular. This could be associated with a corner effect, which creates four secondary flow cells that would oppose liquid drainage at the top of the pipe. Jayanti *et al.* argued that this effect could be particularly strong when a large amplitude "disturbance" wave passes.

Other mechanisms for supporting the liquid layer in horizontal annular flow have been identified: Jacowitz & Brodkey (1964) argued that a circumferential drag on the liquid layer could be due to lift forces on waves. Butterworth (1971) suggested that large amplitude waves (or flow surges) cause a spread of liquid up the wall of the pipe. Laurinat *et al.* (1985) developed a mathematical framework for describing the time-averaged circumferential variation of liquid height which includes the effects of a circumferential component of gas drag, of wave spreading, of gravity and of droplet deposition. They concluded that at low gas velocities, where large amplitude waves do not extend around the whole circumference, the influence of circumferential stresses should be taken into account at the top wall of the pipe. A similar conclusion had been reached by Lin *et al.* (1985). Furthermore, Williams (1990) described a stratified/annular region with a continuous liquid film and no large amplitude waves and Jacowitz & Brodkey (1964) cite instances in which an annular flow has been found with no spray in the gas.

One can conclude from these studies that the transportation of liquid up the wall of the pipe could be associated with large amplitude waves, if they are present (e.g. Fukano & Ousaka 1988; Butterworth 1971; Laurinat *et al.* 1985). In portions of the pipe circumference where large amplitude waves are not present, it seems necessary to take into account a circumferential stress component or to assume that estimations of droplet deposition rates have been too small. The question of whether such stresses in the top part of the pipe would be associated with secondary flows or with some other mechanism, such as wave lift, is still unanswered.

The purpose of this paper is to explore the existence of secondary patterns in gas–liquid flows in a horizontal circular pipe. All of this research was done in a horizontal 9.53 cm pipeline. Contours of constant velocity (isotachs) are constructed from measurement of the magnitude of the streamwise velocity, over the whole pipe cross-section. The method developed by Prandtl (1949) is used to interpret distortions of these isotachs; bulges signify flows away from or toward the wall, depending on their direction.

Two types of experiments were performed. One of these explored the influence of the shape of the cross-section occupied by the gas. Inserts were placed in the bottom of the pipe to mimic a stratified flow. Of interest is the finding that the measured isotachs for a gas flow can be greatly influenced by the fit of the insert at the wall.

In the other experiments isotachs were measured for gas and liquid flowing in a horizontal circular pipe. Superficial gas and liquid velocities of 15–45 and 0.01–0.09 m/s were studied. At low gas velocities a stratified-wavy pattern existed. At intermediate gas velocities atomization occurred and a continuous liquid layer was formed around the pipe circumference. (This is the stratified-annular flow pattern defined by Williams, 1990.) At high gas velocities large amplitude flow surges existed in the liquid layer and extended partially around the pipe circumference.

2. PREVIOUS STUDIES

To the knowledge of the authors, the only other results on secondary flows were reported by Line *et al.* (1991). They studied two conditions, $U_{GS} = 3$ m/s, $U_{LS} = 0.1$ m/s and $U_{GS} = 7$ m/s, $U_{LS} = 0.1$ m/s, for which a stratified flow with no atomization existed. Measurements of two components of the time-averaged velocity were obtained. The study at $U_{GS} = 3$ m/s indicated that a secondary flow did not exist or that it had a very small amplitude. The interface in this case had small waves that were not affecting the drag. At $U_{GS} = 7$ m/s larger waves existed which caused the drag on the gas–liquid interface to be about 8 times larger than on the smooth wall at the top of the pipe. The profile of streamwise velocity at the center plane showed a maximum above the center of the gas space. In the top 70% of the gas space a secondary pattern existed with a downward vertical flow at the vertical center plane and a unidirectional spanwise flow at the horizontal center plane. These results are consistent with the existence of two secondary cells, with centers located above the mid-plane. Two smaller cells, which circulate in the opposite direction could also have existed in the bottom part of the pipe due to non-circularity of the gas space. However, no data were reported to support this notion.

Hanratty & Engen (1957), Cohen & Hanratty (1968) and Miya (1966) measured gas phase velocity profiles at the center plane of a rectangular channel with a 12/1 aspect ratio through which air and water were flowing. Gas velocities from 2 to 14 m/s were studied; the pattern was stratified and waves caused the stress at the gas–liquid interface to be larger than at the gas–solid interface. Measurements of the gas phase velocity showed a distorted profile for which the maximum was displaced away from the wavy interface, toward the top wall. This distortion is explained by an asymmetric distribution of Reynolds stress.

Darling & McManus (1968) observed a displacement of the maximum of the velocity profile in the plane of symmetry toward the bottom of the pipe. This indicated that in the center of the pipe the secondary flow, observed in these studies, was more important in transferring momentum than the Reynolds stresses.

Speziale (1982) suggested that corner effects exist in non-circular pipes because the axial mean velocity gives rise to a non-zero normal Reynolds stress difference in a plane perpendicular to the axial flow direction. Hinze (1967, 1973) has argued that when in a localized region the production is much greater (smaller) than the viscous dissipation, there must be a secondary current that transports turbulence-poor fluid into (out of) this region and turbulence-rich fluid out of (into) the region. He applied this notion to a flow through a rectangular channel having walls of non-uniform roughness. A secondary flow, which moved along the walls from regions with large roughness to regions with small roughness, was found to be superimposed on the corner vortices.

Results by Suzanne (1984, 1985, 1987) and by Fernandez-Flores (1984) for gas and liquid flowing in a stratified pattern in a rectangular channel (with a small aspect ratio) agree with the results of Hinze. The wave height decreased from the lateral walls to the center of the channel. Two large counter rotating vortices, with axes parallel to the primary flow direction, moved along the bottom wall and upward at the center of the channel. It is of interest that the vortical pattern, observed in this investigation, is in the opposite direction of what was found by Line *et al.* (1991) for stratified flow in a circular pipe. (For stratified flow in a circular pipe, the wave height decreases from the centerplane to the wall.)

Jayanti *et al.* (1990b) used a second-order closure model to calculate the secondary flow associated with a decrease in wall roughness from the bottom of a pipe to the top. They predicted two vortices with upward flows at the wall and a downward flow in the center of the pipe.

Thus, a review of the literature shows that the streamwise velocity profile can be distorted due to variations of the Reynolds shear stress and to secondary flows. These secondary flows have been associated with corner effects and with spatial variations of the wall roughness.

3. DESCRIPTION OF EXPERIMENTS

A detailed description of the equipment and the experimental techniques used in this study are contained in a thesis by Williams (1990). The 9.53 cm pipeline is 26 m long. It is constructed with carefully matched flanged plexiglas sections that are 1.5 m long. The test-section, shown in figure 1,

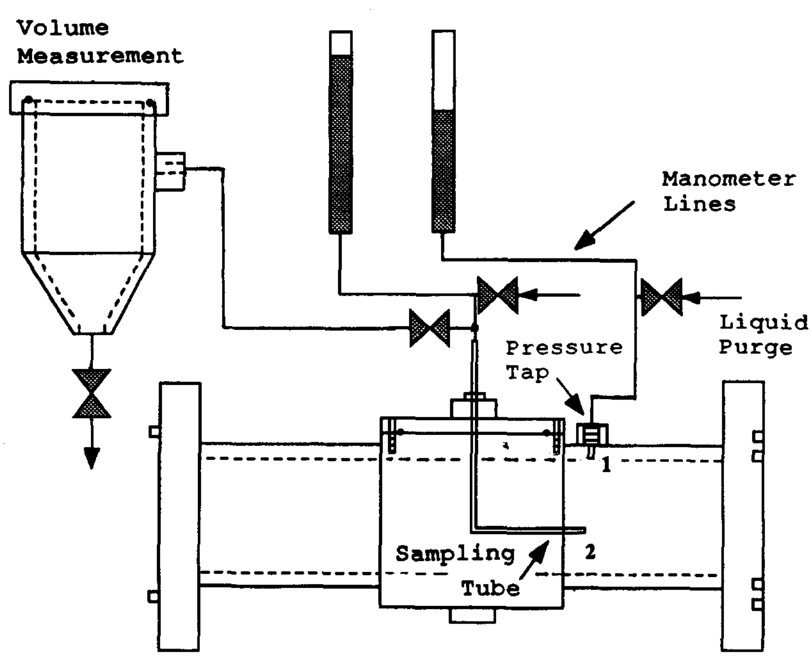

Figure 1. Test section used for velocity and droplet flux measurements.

is located 210 pipe diameters from the inlet. It was machined so that it had a circular cross-section that exactly matched the pipe. An impact tube with internal and external diameters of 0.36 and 0.6 cm measured profiles of the impact pressure and the droplet flux. No difference in the measured droplet flux was obtained with two tubes having inside diameters of 0.36 and 0.63 cm, even though the sampling area varied by a factor of close to four.

Two methods were used to obtain gas velocities. At low gas rates the droplet flux is small. The impact tube contained air; it was cleansed of water with compressed air before a measurement was made. At high gas rates the impact tube was flooded with water, which serves as manometer fluid. The impact pressure at 2 (in figure 1) is measured by the height of the column of liquid in the vertical leg of the impact tube. The static pressure at 1 was determined by measuring the height of liquid in a tube attached to the top of the pipe. The air–water mixture that impacts on the probe opening replenishes any water that is lost from the front of the tube.

Anderson & Mantzouranis (1960) used a momentum balance to derive the following equation that relates the difference in the impact and static pressures, ΔP, to gas velocity, U_G:

$$\Delta P = \tfrac{1}{2}\rho_G U_G^2 + \alpha S U_G G_{LE},$$

where ρ_G is the gas density, G_{LE}, the liquid mass flux and S, the ratio of the velocities of the liquid drops and the gas. The momentum transfer factor, α, depends on the flow pattern of the drops. If they follow the gas streamlines around the probe, $\alpha = 0.5$. For the conditions of the experiments described in this paper the droplets have enough inertia that they move unidirectionally across gas streamlines, so that the capture efficiency of the probe was greater than 99%. Therefore, $\alpha = 1$ was used in the above equation. The relative contributions of the droplets to the impact pressure in the measurements with a flooded tube typically varied between 30 and 70%.

The slip ratio, S, was calculated by integrating the measured gas velocities for different values of the slip ratio until the integrated profile agreed with the measured gas flow rate. To simplify the calculations this slip ratio was assumed to have a constant value over the cross-section of the pipe. Values of S determined by Williams (1990) in this way are plotted in figure 2. The increase of S with increasing gas velocity is expected because of the decrease of drop size. The use of slip ratios which varied linearly with vertical distance in the pipe produced essentially the same velocity measurements as did the assumption of a constant S.

The droplet flux, G_{LE}, was determined by withdrawing liquid through the impact tube, shown in figure 1, and using an area based on the inside diameter. Isokinetic sampling was achieved by applying suction. Detailed descriptions of this technique have been given by Hewitt & Hall-Taylor (1970), Asali *et al.* (1985) and by Williams (1990).

The gas velocity was mapped by measuring five profiles at 0°, 22.5°, 45°, 67.5° and 90° to the vertical. This was accomplished by rotating the test section. Each profile was obtained by making measurements at 19 points separated by a distance of 0.5 cm. The accuracy of the velocity measurements was about 3%.

The liquid level was determined by measuring the resistance between two short parallel chromel wires with a diameter of 0.5 mm and a length of 15 mm. These were contained in a cylindrical plug.

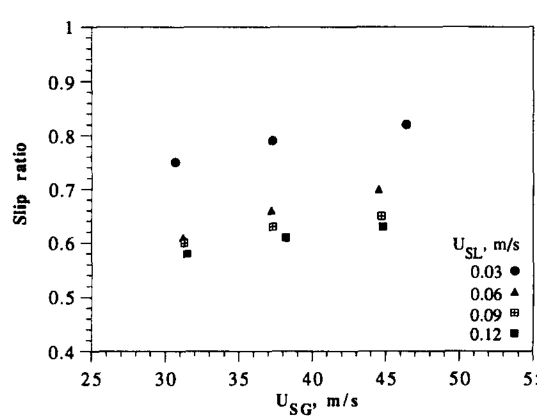

Figure 2. Slip ratios needed to calculate the contribution of droplets to the measured impact pressure.

Table 1. Main parameters and flow conditions

Runs	U_{SG} (m/s)	U_{SL} (cm/s)	U_{max} (m/s)	h_w/D or H/D	Concentration (kg/m^3)	Loading
(a) Two-phase flow with no or a small amount of atomization						
Run 1	14.4	1	18.2	0.04		—
Run 2	23.2	4	28.3	0.1		—
Run 3	17	8	21.1	0.22		—
(b) Two-phase flow with a large amount of atomization						
Run 4	25.3	9	37.3	0.12	0.3	0.2
Run 5	37.2	6	45.8	0.05	0.4	0.3
Run 6	44.5	6	56.6	0.04	0.6	0.4
Run 7	44	9	57.0	0.05	0.7	0.5
Run 8	42.3	3	55.5	0.02	0.2	0.1
(c) Single-phase gas flow in the pipe with insert						
Run 9	22.5	—	27.9	0.13		—
Run 10	24.6	—	30.3	0.25		—
Run 11	20.5	—	25.2	0.15		—

When the liquid level at the bottom of the pipe was large, parallel chromel wires that extended over the whole cross section of the pipe were used. The accuracy of these measurements was about 5% and the minimum value of the film thickness that could be measured was 0.25 mm.

The condition for the various experiments are summarized in table 1. Measurements are presented in table 2. Runs 1, 2 and 3 at superficial gas velocities of 14.4, 23.2 and 17 m/s were done for stratified flows with little or no atomization. Atomization was observed to be initiated close to $U_{SG} = 24$ m/s. Runs 4–8, at superficial gas velocities of 25.3, 37.2, 44.5, 44 and 42.3 m/s, were performed under conditions where a large amount of liquid was entrained in the gas. The reported values of h_W/D are ratios of the tops of the waves at the center plane to the pipe diameter. The average concentrations in table 1 are defined as

$$\langle C \rangle = \frac{1}{(D - h_W)} \int_{h_W}^{D} C \, dy.$$

For the single phase experiments, inserts with $H/D = 0.13$ and 0.25 were screwed into the bottom of the pipe to block off a segment of the pipe. Here H is the height of the insert above the bottom of the pipe and D is the pipe diameter. Values of H/D are also reported in table 1. The length of these inserts was 3 m and velocity measurements were taken 30 pipe diameters downstream.

Table 2. Velocity measurements over the cross-section at conditions which are typical for stratified flow with a negligible (run 3) and a large (runs 4 and 7) amount of atomization. Velocities are given in (m/s) at different angular rotations

	Run 3					Run 4					Run 7				
y/D	0	22.5	45	67.5	90	0	22.5	45	67.5	90	0	22.5	45	67.5	90
0.03	14.1	15.2	16.0	15.8	15.8	28.7	28.5	28.7	28.3	28.3	44.0	43.6	44.6	45.5	46.3
0.08	16.8	17.4	18.0	18.2	18.0	31.3	31.5	32.1	31.7	31.3	49.5	48.4	48.7	49.5	51.2
0.13	17.6	18.2	19.4	19.0	19.4	33.2	33.0	33.5	34.3	35.4	53.0	51.2	53.7	53.4	53.0
0.19	18.2	19.0	20.3	20.5	20.7	34.7	34.7	35.6	36.2	36.5	55.5	54.6	54.6	54.6	55.8
0.24	19.0	19.8	20.5	20.9	21.1	36.2	36.0	36.7	37.1	37.1	56.7	56.3	55.8	55.5	55.8
0.29	19.6	20.3	20.7	21.1	21.1	36.9	36.7	37.3	37.3	37.1	56.9	56.9	56.0	55.8	54.6
0.35	20.3	20.7	20.7	21.1	21.1	37.3	37.3	37.5	37.3	36.5	56.5	56.3	56.0	55.0	54.1
0.40	20.7	21.1	20.7	21.1	21.1	37.3	37.1	36.9	36.7	35.8	55.5	55.2	55.5	54.1	52.9
0.45	21.1	21.1	20.9	20.9	20.7	36.5	36.2	36.5	36.2	35.4	53.7	53.5	53.9	52.9	51.8
0.50	20.7	20.9	20.9	20.7	20.7	35.4	35.2	35.6	35.6	35.4	52.0	52.3	52.0	51.6	51.8
0.56	20.0	20.3	20.7	20.5	20.7	33.9	34.1	34.7	35.4	35.4	50.2	51.8	50.2	51.2	51.8
0.61	18.6	19.2	20.3	20.5	21.1	32.1	32.4	33.5	35.4	35.8	48.0	51.8	48.4	51.2	52.6
0.67	17.1	18.2	19.4	20.5	21.1	30.6	31.3	32.4	35.4	36.2	46.0	51.8	47.8	51.8	53.7
0.72	15.2	16.8	18.6	20.3	21.1	29.2	29.8	31.7	35.2	36.5	44.0	51.8	47.2	52.3	54.5
0.77	12.2	14.5	17.7	19.4	20.9	27.6	28.7	30.6	35.0	36.5	41.0	51.8	46.7	52.3	55.2
0.83			16.8	18.6	20.5	24.6	27.2	28.0	34.5	36.2	35.7	51.8	45.5	52.3	55.2
0.88				17.1	19.6				33.5	35.0		51.2	44.0	51.2	53.4
0.93				15.8	17.7				31.5	32.1		48.9	42.1	47.2	49.8
0.96					16.0				28.5	28.7				44.6	47.2

The studies with inserts were done at gas velocities of 15–48 m/s for which a stratified flow, with or without atomization, would exist. Run 11 is for an insert that was poorly fitted at the tube walls.

4. RESULTS FROM RUNS WITH NEGLIGIBLE ATOMIZATION

Figure 3 shows typical vertical velocity profiles at the center plane of the gas space under conditions for which little or no atomization occurred, where y is the distance from the bottom wall. The experiments at three different superficial gas velocities, $U_{SG} = 14.4$, 23.2 and 17 m/s were conducted with superficial liquid velocities of $U_{SL} = 1$, 4 and 8 cm/s. The lines in the figure represent the top of the waves. In all three experiments large amplitude waves existed so that the interfacial drag at the bottom of the gas space was much larger than at the top. If no secondary flow existed one would expect the maximum in the velocity to be located above the midpoint of the gas space.

Figure 3(a) shows that the maxima are displaced downward and that an inflection point existed in the top parts of the velocity profiles. An approximate similarity in these profiles is observed if the vertical coordinate is normalized with the length of the gas space between the tops of the waves, h_w, and the top of the pipe and if the velocity is normalized by the maximum value. This is shown in figure 3(b). The maximum is seen to be located at $0.60 < y/(D - h_w) < 0.65$. These results clearly indicate the existence of a secondary flow.

Velocity isotachs for runs 1, 2 and 3 are shown in figure 4, where the velocities are normalized by the maximum value. The dotted curve indicates the approximate average location of the interface. The use of the method of Prandtl indicates a secondary pattern in the top part of the pipe with a downward flow at the center plane and an upward flow at the wall. There is a decrease in wave roughness from the center plane to the pipe wall, therefore this secondary flow could be associated with a spatial variation in wall roughness.

The upward bulges in the bottom part of the gas space are more difficult to interpret. One possibility is the existence of an asymmetric distribution of Reynolds stresses along the center plane

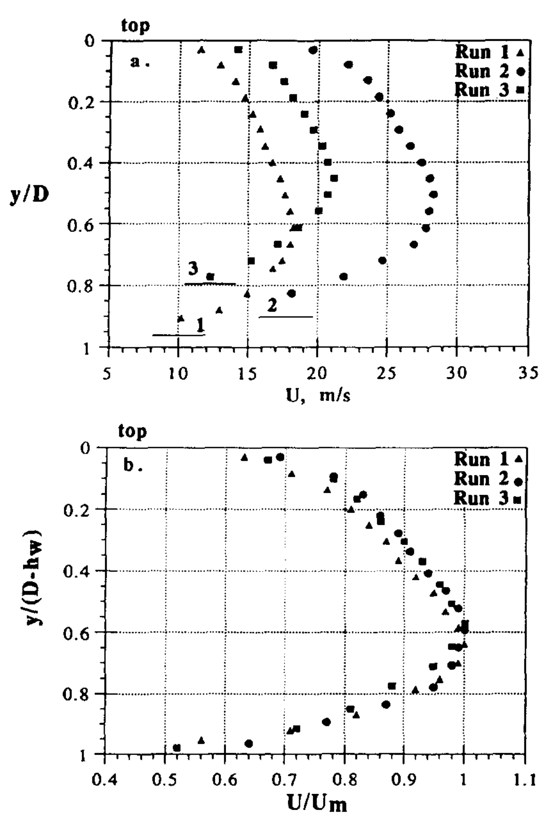

Figure 3. Regular (a) and normalized (b) vertical velocity profiles for conditions with no or a small amount of atomization. See table 1 for flow conditions.

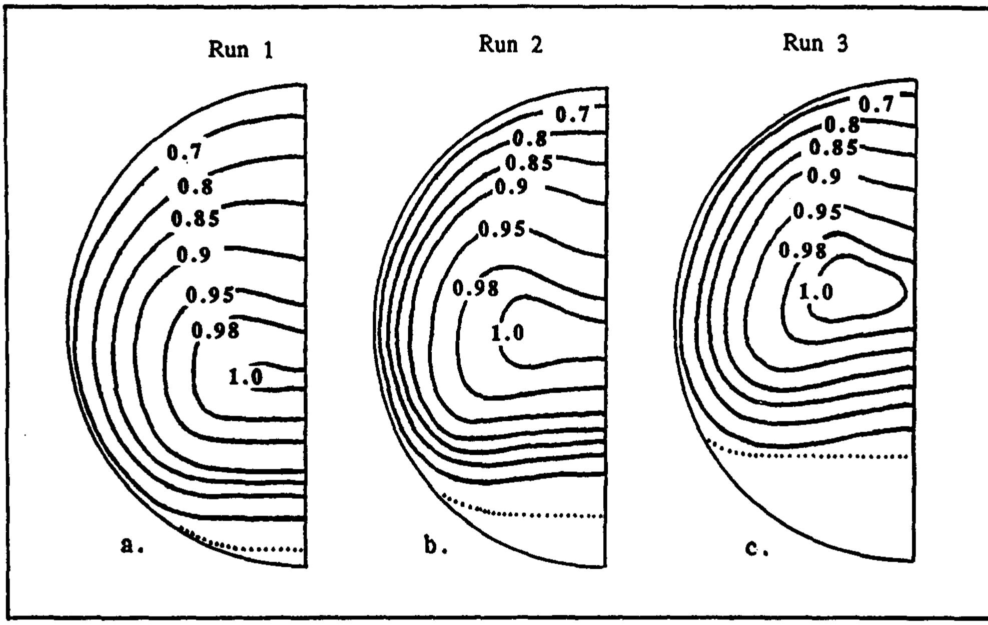

Figure 4. Velocity contours (isotachs) for conditions with no or a small amount of atomization (normalized with the maximum velocity). See table 1 for flow conditions.

caused by the much greater gas phase drag at the gas–liquid interface than at the top of the pipe. Another possibility is that the secondary pattern consists of at least four cells. This arises because a pair of corner eddies is superimposed on the pattern associated with roughness variations. The changes of the isotachs and the increased stretching of the isotachs toward the corner with increasing liquid height (shown in figure 4), then, could be interpreted as resulting from an increase in the intensity of this "corner effect".

The contributions of Reynolds stress and secondary flow to the transport of momentum along the center plane are, respectively, $\partial(\overline{u'v'})/\partial y$ and $\partial(\bar{U}\bar{V})/\partial y$, where u', v' are the fluctuating components and $\bar{U}$, $\bar{V}$ are mean velocities. Usually v' is approximately equal to $\bar{V}$ and $\bar{U}$ is an order of magnitude larger than u'. Consequently, secondary flows are expected to control momentum transport, when they are present. The second interpretation presented above, therefore, seems the more plausible.

5. RESULTS OF STUDIES WITH INSERTS

Some help in understanding the velocity measurements in figures 3 and 4 can be obtained from studies with inserts.

Figure 5(a) and (b) shows isotachs which supposedly approximate the gas space over idealized stratified flows. The velocity measurements are made dimensionless with the maximum value. When plotted in this form no detectable effect of gas velocity could be found for superficial velocities from 15 to 48 m/s.

The isotachs are similar for the two inserts shown in figure 5(a) and (b). They are approximately parallel to the pipe wall in the space enclosed by dotted lines at the top of the gas space. The small distortion of the isotachs around the corner suggests the existence of corner vortices of the type observed in non-circular ducts. Their influence appears to be limited to the corner region so that the maximum velocity in the center plane is located in the middle of the gas space. The decrease in the size of the region where isotachs are parallel to the wall indicates that the influence of the corner vortices increases in extent as the ratio H/D increases.

A comparison of the isotachs in figure 4 with those in figure 5(a) and (b) indicates that the corner effects are much stronger for a gas–liquid flow. The "corner" for a gas–liquid stratified flow at large gas velocities is different from what is studied in figure 5(a) and (b). As sketched in figure 4 increases in gas velocity cause the liquid to climb farther up the wall. This wavy film agitates the gas flow

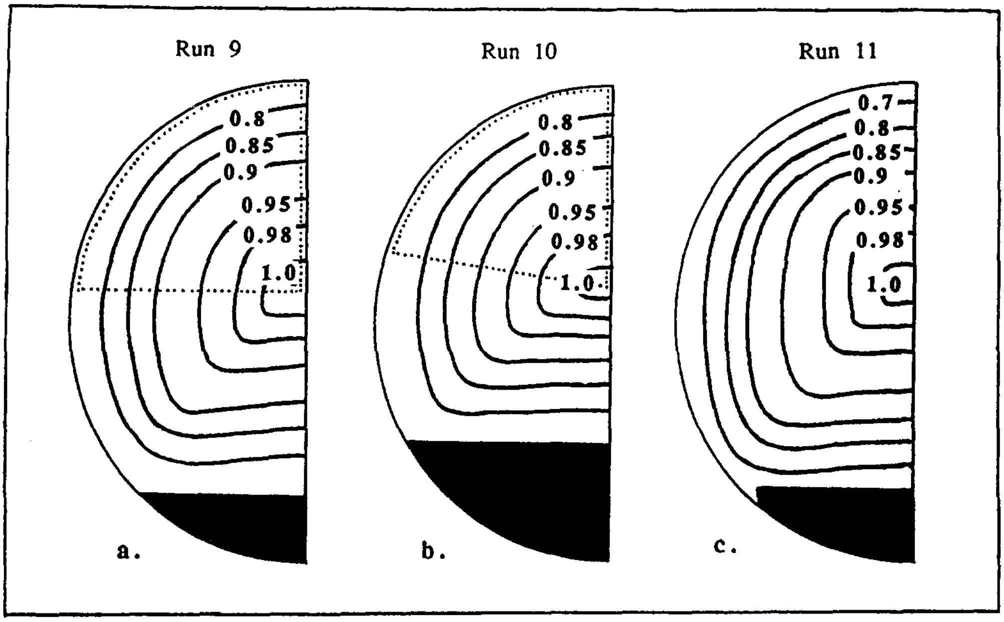

Figure 5. Velocity contours (isotachs) in a circular pipe with inserts (normalized with the maximum velocity). See table 1 for flow conditions.

by oscillating up and down. Thus, the "corner" in an actual stratified flow at high gas velocities could be a source of turbulence.

Figure 5(a) and (c) compares isotachs obtained with a tight fit at the corner to those obtained with a 0.2 cm gap at the corner. The results were obtained in several different experiments over a range of gas velocities. The distortion of the isotachs in figure 5(c) indicates much stronger corner vortices than are observed with tightly fitted inserts. The isotachs in the upper part of the gas space in figure 5(c) are not concentric with the wall of the pipe. The existence of strong circulation patterns with an upward flow in the center plane at the bottom of the gas space and a downward flow at the top of the gas space is suggested.

A comparison of figure 5(c) with figure 4(b) shows a similarity between measurements with poorly fitted inserts and gas–liquid flows.

6. RESULTS FOR STRATIFIED FLOWS WITH SIGNIFICANT ATOMIZATION

Figure 6(a) presents velocity profiles measured at the vertical center plane with large gas velocities and large entrainment in the gas. The lines at the bottom of the figure are the approximate locations of the wave crests. Runs 4, 5, 6 and 7 are plotted in dimensionless form in figure 6(b). In all of these the maximum is displaced to the upward part of the gas space, in contrast to experiments with no entrainment in figure 3. These results suggest that the presence of entrainment causes a circulation cell with downward flow at the wall and upward flow at the center. This is supported by the plots of isotachs for runs 4 and 7 shown in figure 7(a) and (b).

A comparison of results for runs 6 and 7 in figure 6(a), at approximately the same gas velocity, shows an increase in the upward displacement of the maximum velocity with increasing liquid flow, or increasing liquid entrainment. A comparison of experiments at the same liquid flow but at different gas rates (runs 4, 7 and 5, 6) also show an increase in the upward displacement with increasing drop concentration (see table 1).

Tsuji & Morikawa (1982) observed an upward displacement of the maximum in the gas-phase velocity profile in their studies of air–solid flow in a 3.0 cm horizontal pipe, which seems to be associated with a suppression of turbulent transport because of density stratification. Particle diameters of 0.2 and 3.4 mm and a range of gas velocities from 6 to 20 m/s were studied. The displacement was found to increase with an increase in the loading, defined as the ratio of mass flow rate of the solids to the mass flow rate of the gas.

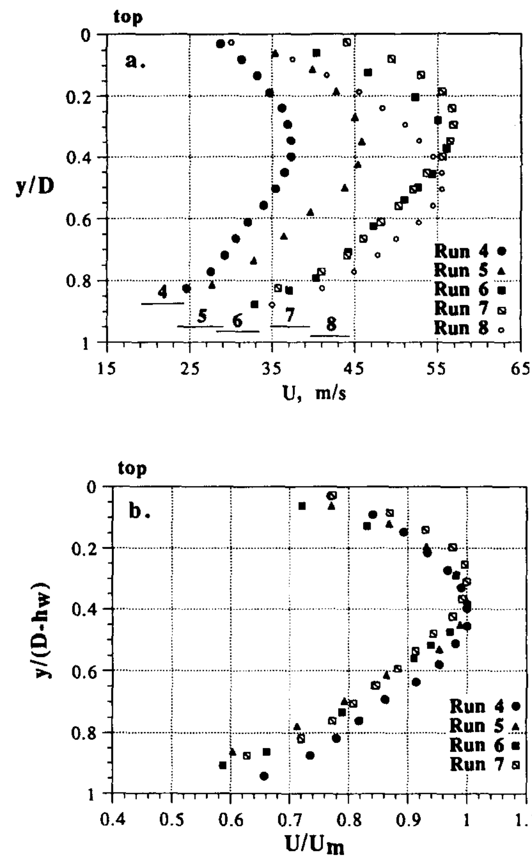

Figure 6. Regular (a) and normalized (b) vertical velocity profiles for conditions with a large amount of atomization. See table 1 for flow conditions.

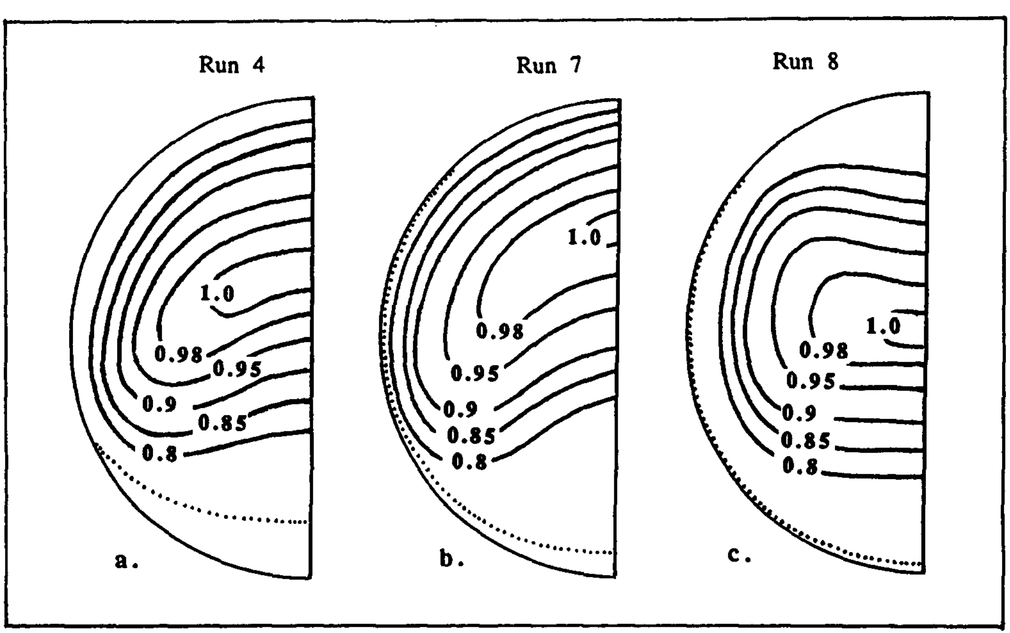

Figure 7. Velocity contours (isotachs) for conditions with a large amount of atomization (normalized with the maximum velocity). See table 1 for flow conditions.

From table 1 it can be seen that, under conditions of large atomization, the loading varied from 0.1 (run 8) to 0.5 (run 7). Most of the experiments by Tsuji & Morikawa were performed at higher mass ratios. Their results for a loading 0.4 showed a very small upward shift in the maximum velocity. Distortions similar to what is shown in figure 6 required loadings in solid–liquid flows that are an order magnitude larger than existed in the annular flows. This suggests that suppression of mixing due to density stratification cannot explain the results shown in figure 6.

A possible interpretation of these results is that density gradients associated with spatial variations of droplet concentration in the horizontal direction provide pressure gradients that drive a secondary flow. Some support for this interpretation is presented in figure 8 which gives contours of constant droplet concentration for run 7. Values of concentration are normalized with the maximum value that was found near the bottom. The dot in this figure indicates the extent of the disturbance waves at the side wall. The atomization from those waves provides a larger concentration (or larger density) near the wall; this is consistent with the existence of a downward flow at the wall. The shape of the contours also suggests an upward flow in the center plane.

An interesting, intermediate case is run 8, which was carried out at a high gas velocity but at a small liquid flow. Under such conditions entrainment is low, but significant. As can be seen in figures 6(a) and 7(c), the maximum velocity is located, approximately, in the center of the gas space, in contrast to runs 4–7. Run 8 also differs from run 2 (in figure 3), at approximately the same liquid flow but with a lower gas velocity and negligible entrainment. This suggests that pressure gradients associated with the presence of droplets in the gas phase (in run 8) appear to just counterbalance the stresses causing the secondary flow indicated in figure 4.

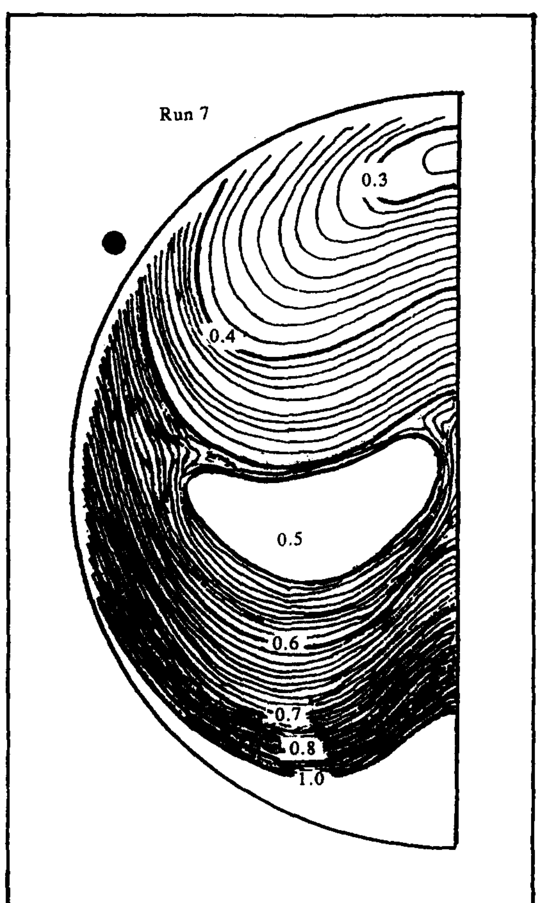

Figure 8. Contours of concentration for conditions with a large amount of atomization (run 7). See table 1 for flow conditions. The dot indicates the extent of disturbance waves at the side wall. The concentrations are normalized with the maximum value.

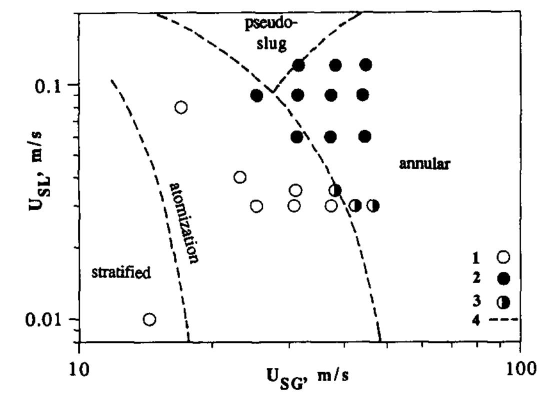

Figure 9. Map characterizing the displacement of maxima in the velocity profile: 1, below the center of gas space; 2, above the center; 3, at the center. The dashed curves (4) separate flow regimes defined by Lin & Hanratty (1987).

7. DISCUSSION

Secondary flows in the gas phase are not important for stratified flows in which only small amplitude waves exist at the interface. However, at high gas velocities large amplitude waves are generated and a secondary flow exists which causes a downward displacement of the maximum velocity, just the opposite of what is found for single phase flow through a channel with a roughened bottom wall and a smooth top wall.

This secondary flow consists of two or more cells. It is believed to be associated mainly with a decrease in the wave roughness from the center of the pipe to the wall and with corner effects. This indicates that for a two-phase flow pattern, the secondary flow structure is more complicated than was suggested by Pletcher & McManus from single phase experiments with a roughness variation. The corner effects appear to be much stronger than would exist because of a non-circular gas space. This could result from disturbances introduced at the corners by the intermittent motions of the liquid layer which climbs up the side walls of the pipe.

When the gas velocity is large enough atomization occurs from the sides, as well as the bottom, of the pipe. This causes horizontal gradients in droplet concentration. Pressure gradients in the gas associated with these gradients would favor a secondary flow that is upward at the center plane and downward at the walls. At low drop concentrations this would counterbalance the secondary flow associated with roughness variation. At large drop concentrations a strong secondary flow exists which displaces the maximum velocity upward and transports drops toward the top wall at the center plane.

Figure 9 summarizes the results presented in this paper and in the thesis of Williams (1990). The open (1) and closed (2) points, respectively, represent conditions for which the maximum velocity is displaced downward or upward. Partially filled symbols (3) indicate that the velocity maxima is located in the middle of the gas space. The comparison with flow regime transitions (4), defined by Lin & Hanratty (1987), shows that annular flow occurs when the secondary flow is controlled by gradients of droplet concentration.

Secondary flows in the gas phase affect the spatial variation of mean velocity and of droplet concentration. Under conditions of large entrainment interfacial stresses associated with the secondary flow would aid the drainage of the liquid film on the wall. However, the secondary flow would also tend to increase the thickness of the liquid film by enhancing the transport of liquid drops the top wall. Under conditions of very small entrainment the secondary flow would oppose the drainage of liquid and the transport of drops to the top wall.

An exact assessment of the importance of these effects on the variation of the thickness of liquid layer around the pipe circumference cannot be made, at this time, because quantitative definitions of the various factors outlined in the Introduction are not available.

Acknowledgements—This work has been supported by the Shell Development Company and the Department of Energy under Grant DOE DEFGO2-86ER 13556.

REFERENCES

ANDERSON, G. H. & MANTZOURANIS, B. G. 1960 Two-phase (gas–liquid) flow phenomena–I. *Chem. Engng Sci.* **12,** 109–126.

ASALI, J. S., LEMAN, G. M. & HANRATTY, T. J. 1985 Entrainment measurements and their use in design equations. *PCH Phys.-Chem. Hydrodynamics* **6,** 207–221.

BUTTERWORTH, D. 1971 Air–water annular flow in a horizontal tube. UKAEA Report No. AERE-R6687.

COHEN, L. S. & HANRATTY, T. J. 1968 Effect of waves at a gas–liquid interface on a turbulent air flow. *J. Fluid Mech.* **31,** 467–479.

DARLING, R. S. & MCMANUS, N. H. 1968 Flow patterns in circular ducts with circumferential variation of roughness: a two-phase flow analogue. *Proc. 11th Mid-Western Mechanics Conf.* **9,** 153–163.

FERNANDES-FLORES, R. 1984 Etudes des interactions dynamiques en ecoulement diphasique stratifie. These de Docteur Ingenieur, INPT.

FUKANO, T. & OUSAKA, A. 1989 Prediction of the circumferential distribution of film thickness in horizontal and near-horizontal gas–liquid annular flows. *Int. J. Multiphase Flow* **15,** 403–419.

HEWITT, G. F. & HALL-TAYLOR, N. S. 1970 *Annular Two-phase Flow.* Pergamon Press, Oxford.

JACOWITZ, L. A. & BRODKEY, R. S. 1964 An analysis of geometry and pressure drop for the horizontal, annular, two-phase flow of water and air in the entrance region of a pipe. *Chem. Engng Sci.* **19,** 261–274.

JAYANTI, S., HEWITT, G. F. & WHITE, S. P. 1990a Time-dependent behavior of the liquid film in horizontal annular flow. *Int. J. Multiphase Flow* **16,** 1097–1116.

JAYANTI, S., WILKES, N. S., CLARKE, D. S. & HEWITT, G. F. 1990b The prediction of turbulent flows over roughened surface and its application to interpretation of mechanisms of horizontal annular flow. *Proc. R. Soc. Lond.* **431,** 71–88.

HANRATTY, T. J. & ENGEN, J. M. 1957 Interaction between a turbulent air stream and a moving water surface. *AIChE Jl* **3,** 299–304.

HINZE, J. O. 1973 Experimental investigation on secondary currents in the turbulent flow through a straight conduit. *Appl. Sci. Res.* **28,** 453–465.

LAURINAT, J. E., HANRATTY, T. J. & JEPSON, W. P. 1985 Film thickness distribution for gas–liquid annular flow in a horizontal pipe. *PCH Phys.-Chem. Hydrodynamics* **6,** 179–195.

LIN, P. G. & HANRATTY, T. J. 1987 Effect of pipe diameter on flow patterns for air–water flow in horizontal pipes. *Int. J. Multiphase Flow* **13,** 549–563.

LIN, T. F., JONES, O. C., LAHEY, R. T., BLOCK, R. S. & MIRASE, M. 1985 Film thickness measurements and modelling in horizontal annular flows. *PCH Phys.-Chem. Hydrodynamics* **6,** 197–205.

LINE, A., MASBERNAT, L., MIRE, A. & SOUALMIA, A. 1991 Analysis of the local structure of co-current stratified two-phase flow. *European Two-phase Flow Group Meeting,* Rome.

MIYA, M. 1966 Effect of waves on turbulence. M.Sc. dissertation, University of Illinois, Urbana, IL.

NIKURADZE, J. 1930 Turbulente stromung in nichtkreisformigen rohre. *Ing.-Arch.* **1,** 306–332.

PLETCHER, R. H. & MCMANUS, H. N. 1965 The fluid dynamics of three-dimensional liquid films with free-surface shear: a finite difference approach. In *Proc. 9th Mid-Western Mechanics Conf.,* WI.

PRANDTL, L. 1927 Turbulent flow. NASA TM, 435.

SPEZIALE, C. G. 1982 On turbulent secondary flows in pipes of noncircular cross-section. *Int. J. Engng Sci.* **20,** 863–872.

SUZANNE, C., FABRE, J., MASBERNAT, L. & MARODON, D. 1984 Turbulent structure of wavy stratified air–water flows. In *Gas Transfer at Water Surfaces* (Edited by BRUTSAERT, W. & JIRKA, G. H.). Reidel, Dordrecht.

SUZANNE, C. 1985 Structure de l'ecoulement stratifie de gas et de liquide en canal rectangulaire. These d'Etat, INPT.

SUZANNE, C., FABRE, J. & MASBERNAT, L. 1987 Stratified flow, Part 1: local structure. In *International Workshop on Two-phase Flow Fundamentals* (Edited by HEWITT, G. F., DELHAYE, J. M. & ZUBER, N.). Hemisphere, London.

WILLIAMS, L. R. 1990 Effect of pipe diameter on horizontal annular two-phase flow. Ph.D. dissertation, University of Illinois, Urbana, IL.